Supplementary Material for "Frictional Effects on Shear-Induced Diffusion in Suspensions of Non-Brownian Particles"

Han Zhang, Dmitry I. Kopelevich, and Jason E. Butler

S1 Sensitivity to Model Parameters

Lubrication Range. To examine the effect of lubrication range on shear-induced diffusion, simulations of frictionless particles with different lubrication cut-off distance were performed. As shown in figure S1, the lubrication range has a relatively small impact on diffusion of particles in a dense suspension.

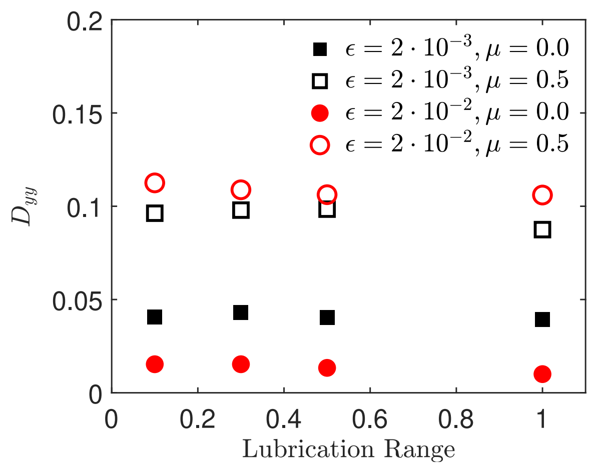

Figure S1: Effect of the lubrication cut-off distance on particle diffusivity in a suspension with volume fraction $\phi = 0.45$.

Elastic Force Constant k_n. In the current work, the value of k_n is given by $k_n = (2\delta)^{-3/2}$, where $\delta = 0.05\epsilon$. This value of δ is rather arbitrary. In section 3.1, we demonstrated that offsets in pairwise collisions of particles in a dilute suspension are not sensitive to the specific value of δ. Figure S2 shows that sensitivity of particle diffusivity in a dense suspension to δ is also weak. For frictionless particles as well as smooth ($\epsilon = 2 \cdot 10^{-3}$) frictional particles, the diffusivity is essentially independent of δ. For rough ($\epsilon = 2 \cdot 10^{-2}$) frictional particles the diffusivity exhibits a weak dependence on δ at small δ.

Note that only diffusivities for $\delta \leq 0.15\epsilon$ are computed, since increasing δ beyond 0.15ϵ leads to particle overlaps in dense suspensions. This is evident from the roughness deformation $\tilde{\epsilon} = 1 - h/2\epsilon$ shown in table S1. While the average roughness deformation $\langle\tilde{\epsilon}\rangle$ remains

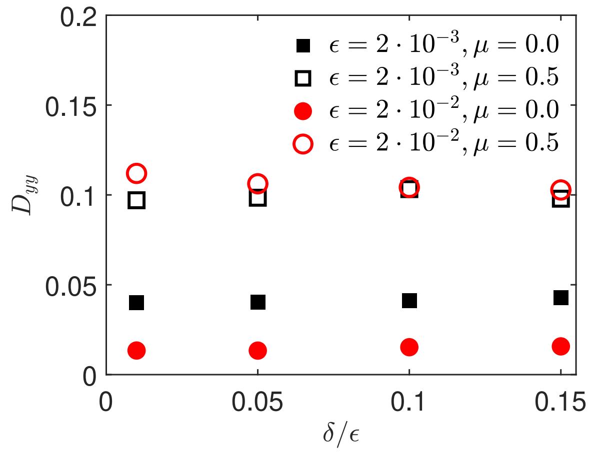

Figure S2: Effect of the elastic force constant k_n on particle diffusivity in a suspension of volume fraction $\phi = 0.45$. To facilitate comparison between particles of different roughness, the x-axis of the plot shows the parameter δ corresponding to $k_n = (2\delta)^{-3/2}$.

Table S1: Effect of δ on roughness deformation $\tilde{\epsilon} = 1 - h/2\epsilon$ in a dense ($\phi = 0.45$) suspension of frictionless ($\mu = 0.0$) particles with two different values of roughness ϵ. Average and maximum roughness deformations, $\langle\tilde{\epsilon}\rangle$ and $\tilde{\epsilon}_{\max}$, are shown.

δ/ϵ	$\langle\tilde{\epsilon}\rangle$		$\tilde{\epsilon}_{\max}$	
	$\epsilon = 2 \cdot 10^{-3}$	$\epsilon = 2 \cdot 10^{-2}$	$\epsilon = 2 \cdot 10^{-3}$	$\epsilon = 2 \cdot 10^{-2}$
0.01	0.022	0.015	0.125	0.103
0.05	0.110	0.073	0.725	0.460
0.1	0.217	0.148	0.999	0.925
0.15	0.323	0.223	1.000	1.000

relatively small at $\delta = 0.15\epsilon$, the maximum deformation $\tilde{\epsilon}_{\max}$ approaches 1, which indicates that further increase of δ will lead to particle overlap.

Tangential Spring Constant k_t. In the current work, we use the classical choice (Shäfer *et al.*, 1996; Silbert *et al.*, 2001; Gallier *et al.*, 2014) for the value of the tangential spring stiffness, $k_t = mk_n(2\delta)^{1/2}$ with $m = 2/7$. It is shown in section 3.2 that k_t has a negligible effect on particle offsets in pairwise collisions in a dilute suspension. Figure S3 shows that k_t also has a small effect on particle diffusivity in dense suspensions, as long as k_t is sufficiently large. Specifically, dependence of D_{yy} on k_t is weak for $m \geq 2/7$. On the other hand, diffusivity is sensitive to k_t for $m < 2/7$.

S2 Additional Information on Effects of Friction on Pairwise Collisions

Trajectories of pairwise collisions of frictional and frictionless particles are shown in figure S4. It is evident that there is essentially no difference between the trajectories followed

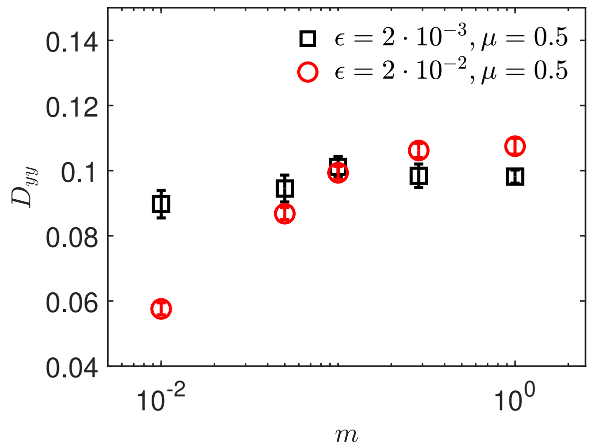

Figure S3: Effect of the parameter m determining the tangential spring constant $k_t = mk_n(2\delta)^{1/2}$ on particle diffusivity in a suspension of volume fraction $\phi = 0.45$ and the elastic constant k_n corresponding to $\delta = 0.05\epsilon$.

by the particles (see figure S4a) and a very small difference in the time required to complete the trajectory (see figure S4b).

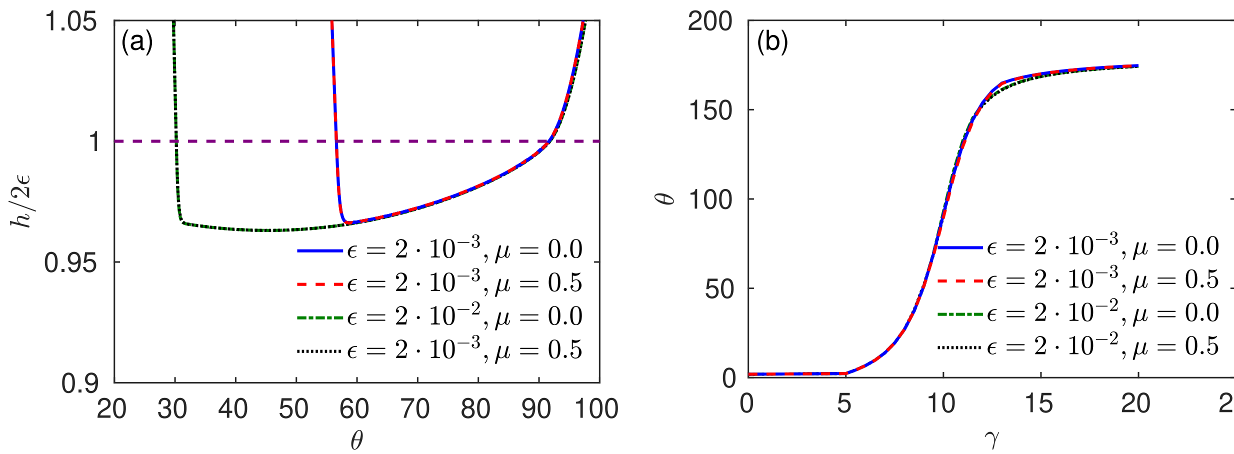

Figure S4: Examples of pairwise collisions of particles with and without friction: (a) particle trajectories; the dashed magenta line shows the border between reversible and irreversible segments of the trajectories; (b) dependence of the angle θ on the strain γ.

S3 Scaling of the Mean-Squared Displacement with Strain

To confirm that the particle dynamics is diffusive, the mean-squared displacement $\langle(\Delta y)^2\rangle$ was fitted to the power law

$$\langle(\Delta y)^2\rangle \propto \gamma^{\alpha}. \tag{S1}$$

Estimates of strains γ_0 required to reach the power law dependence, as well as the values of the exponent α are summarized in table S2. The values of α are very close to 1, thus confirming diffusive behavior. We note that frictionless particles tend to take longer to reach diffusive behavior than fricional particles.

Table S2: Power law exponents α for the dependence of the mean square displacement $\langle(\Delta y)^2\rangle$ on strain γ and the values γ_0 of strain at which $\langle(\Delta y)^2\rangle$ is considered to have reached the power-law dependence on γ.

ϕ	ϵ	μ	α	γ_0
0.25	$2 \cdot 10^{-3}$	0	0.97 ± 0.04	70
	$2 \cdot 10^{-3}$	0.5	0.92 ± 0.02	30
	$2 \cdot 10^{-2}$	0	0.97 ± 0.07	70
	$2 \cdot 10^{-2}$	0.5	1.05 ± 0.04	30
0.35	$2 \cdot 10^{-3}$	0	0.95 ± 0.03	30
	$2 \cdot 10^{-3}$	0.5	0.94 ± 0.02	30
	$2 \cdot 10^{-2}$	0	0.92 ± 0.05	70
	$2 \cdot 10^{-2}$	0.5	1.01 ± 0.03	30
0.45	$2 \cdot 10^{-3}$	0.0	1.01 ± 0.03	30
	$2 \cdot 10^{-3}$	0.25	0.99 ± 0.02	30
	$2 \cdot 10^{-3}$	0.5	1.02 ± 0.03	30
	$2 \cdot 10^{-3}$	1.0	1.01 ± 0.04	30
	$2 \cdot 10^{-3}$	1.5	1.01 ± 0.02	30
	$2 \cdot 10^{-2}$	0.0	0.99 ± 0.04	70
	$2 \cdot 10^{-2}$	0.25	1.02 ± 0.03	30
	$2 \cdot 10^{-2}$	0.5	1.00 ± 0.01	30
	$2 \cdot 10^{-2}$	1.0	0.98 ± 0.02	30
	$2 \cdot 10^{-2}$	1.5	1.01 ± 0.02	30

S4 Comparison with Simulations that Include Long-Range Hydrodynamic Interactions

The model considered in the current work neglects long-range hydrodynamic interactions. In this section, we test this assumption by comparing our simulations with Stokesian dynamics simulations of Sierou & Brady (2004), which include the long-range interactions To facilitate the comparison, simulations reported in this section neglect friction and utilize the same normal contact force model as was used by Sierou & Brady (2004),

$$\boldsymbol{F}_{\alpha\beta}^{(C,n)} = \frac{e^{-\tau h_{\alpha\beta}}}{1 - e^{-\tau h_{\alpha\beta}}} \boldsymbol{n}_{\alpha\beta}. \tag{S2}$$

Here, τ determines the range of the force and is set to 1000.

Diffusivities obtained from our simulations are compared with the Stokesian dynamics results of Sierou & Brady (2004) in figure S5. It is evident that, for sufficiently high volume fractions ($\phi \geq 0.2$), contribution of long-range interactions to diffusivity is negligible.

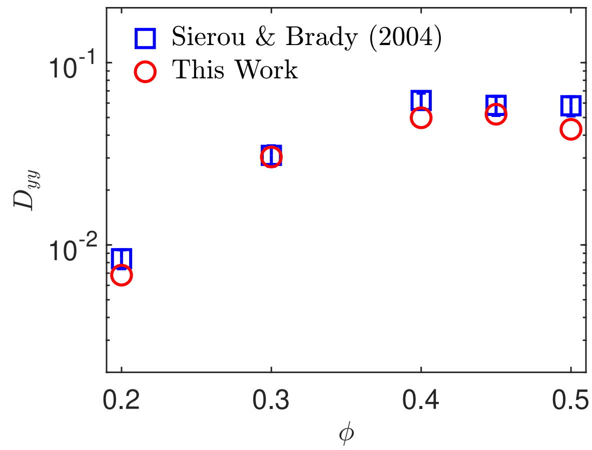

Figure S5: Comparison of diffusivity of frictionless particles obtained from our simulations neglecting long-range interactions with the results of the Stokesian dynamics simulations of (Sierou & Brady, 2004). Both sets of simulations use the contact force given by (S2).

References

Gallier, S., Lemaire, E., Peters, F. & Lobry, L. 2014 Rheology of sheared suspensions of rough frictional particles. *J. Fluid Mech.* **757**, 514–549.

Shäfer, J., Dippel, S. & Wolf, D. 1996 Force schemes in simulations of granular materials. *Journal de Physique I* **6** (1), 5–20.

Sierou, A. & Brady, J. F. 2004 Shear-induced self-diffusion in non-colloidal suspensions. *J. Fluid Mech.* **506**, 285–314.

Silbert, L. E., Ertaş, D., Grest, G. S., Halsey, T. C., Levine, D. & Plimpton, S. J. 2001 Granular flow down an inclined plane: Bagnold scaling and rheology. *Phys. Rev. E* **64**, 051302.